

On the physical origin of enhanced turbulent-dispersion of inertial particles in boundary layer flows

J. Chauchat, D. Hurther, and T. Revil-Baudard
Univ. Grenoble Alpes, CNRS, Grenoble INP, LEGI, 38000 Grenoble,
 France* Institute of Engineering Univ. Grenoble Alpes*

Z. Cheng
*Civil and Environmental Engineering, Center for Applied Coastal Research,
 University of Delaware, Newark, DE 19711, USA
 Now at Convergent Science Inc., Madison, WI 53719, USA*

T.-J. Hsu
*Civil and Environmental Engineering, Center for Applied Coastal Research,
 University of Delaware, Newark, DE 19711, USA **

One of the most enigmatic science question concerning inertial particle transport by a turbulent boundary layer flow is the value of the turbulent Schmidt number as the ratio of particle diffusivity and turbulent eddy viscosity. Using direct acoustic measurement of turbulent particle flux profile, and two-phase flow turbulence-resolving numerical simulation, it is demonstrated that turbulent dispersion of particles is reduced rather than enhanced when predicted with existing literature model. The explanation lies in the misleading assumption of settling velocity in quiescent water to estimate the turbulent particle diffusivity while direct measurements and simulations of turbulent particle flux support the occurrence of settling retardation.

The transport of solid particles by a turbulent fluid flow is a key process in geophysical and industrial two-phase flows such as material and food processing, pneumatic transport, fluidized beds, slurry flows or sediment transport. In all these situations, interactions between particles and fluid turbulence are key processes that contribute to the dynamics of the system. Among the consequences induced by the presence of particles the modification of fluid turbulence and the turbulent dispersion of particles are crucial mechanisms [1]. A further complexity arises when particles are inertial, *i.e.* when the particle response time τ_p is larger than a representative turbulent eddy time-scale τ_f , inducing that the Stokes number $St = \tau_p/\tau_f$ is greater than unity. Inertial particles act as a local filter for the turbulent kinetic energy spectrum due to their not fully correlated movements with turbulent eddies of smaller size than the particle itself. This problem has been studied in many different flow configurations including Homogeneous Isotropic Turbulence, jets and turbulent wall-bounded flows such as closed or free-surface pipe, duct and open-channel flows.

In sediment transport, under intense flow conditions, particles are locally eroded from the underlying granular bed and transported into suspension by turbulent eddies [2]. The coupling between the sediment flux and the underlying bed topography controls the large-scale morphological evolution of rivers, estuaries and coastal nearshore zones [3]. In most of these situations, the transported particles are made of inorganic non-cohesive sand grains with Stokes number values well above unity, *i.e.*

inertial particles. In the context of climate change, erosion associated with extreme events such as river floods and coastal storms are found to increase in intensity and frequency. Sediment transport is a truly multi-scale process coupling fine scale turbulence-particle interactions ($O(\mu m)$ - $O(ms)$) with the morphological evolution of natural systems at large scales ($O(km)$ - $O(yrs)$). Therefore, elucidation of the governing interaction processes associated with the transport of inertial particles by a turbulent boundary layer flow is a major scientific issue.

The particle flux, defined as the integral over the flow depth of the product between the local velocity and particle concentration, is the quantity of interest. Consequently, a better understanding of the fine-scale processes that control both the concentration and velocity profiles through turbulent dispersion and turbulence modifications of the boundary layer, is the nub of the problem. Turbulence modifications may modify the von Karman constant κ in the Prandtl mixing length model [4]. Vanoni [5] reported significantly altered values of κ as low as 0.3 (compared to the universal value of 0.41 for clear-water boundary layer flows) for turbulent suspension of fine sands in an open-channel flow. Moreover, the turbulent diffusivity of inertial particles may differ from that of fluid parcels or passive tracers which is characterized by the turbulent Schmidt number S_e , as the ratio between turbulent diffusivity of particle concentration ϵ_ϕ and the eddy-viscosity ν^t . Since the seminal work of Rouse [6], due to the measurement difficulty, very few experimental studies have addressed the value of the turbulent Schmidt number in particle-laden flows [7–10]. Existing data synthesized by Lyn [11] reveal values both lower and higher than unity with a large scatter (see figure 1).The goal

* julien.chauchat@univ-grenoble-alpes.fr

of the present contribution is to explain the large scatter in turbulent Schmidt number values and to provide a physical explanation for the contradictory findings in the literature.

Here, using the recent high-resolution experimental data-set of [12, 13] and turbulence-resolving two-phase flow simulations of [14], we demonstrate that the uncertainties on the value of turbulent Schmidt number can be explained by a shortcoming in the methodology. It can be deduced that the real values of the turbulent Schmidt number based on directly measured turbulent particle fluxes is higher than unity for inertial particles. The physical explanation for this controversy is due to settling retardation effects. Beyond sediment transport, this result opens new perspectives for other applications such as pollutants transport in the atmosphere, particle deposition in materials processing or pneumatic transport of granular materials.

In the classical sediment transport approach, suspended-load under steady turbulent flow conditions is modeled following Rouse [6] by assuming a local balance between a downward gravity-driven settling flux $W_s \langle \phi \rangle$ and an upward turbulent dispersion flux $\langle w' \phi' \rangle$ (also called Reynolds particle flux in the following see appendix A for details) where W_s is the settling velocity of a single particle approximated by its value in quiescent water W_s^0 , $\langle \rangle$ denote a temporal averaging operator and $'$ the associated turbulent time fluctuating component after application of a local Reynolds decomposition. Rouse [6] proposed to model the Reynolds particle flux using a gradient diffusion model as:

$$\langle w' \phi' \rangle = -\epsilon_\phi \frac{d\langle \phi \rangle}{dz}, \quad (1)$$

with $\epsilon_\phi = \nu^t / S_c$.

Using Prandtl's law-of-the-wall and associated logarithmic mean velocity profile in the bottom boundary layer, it is possible to analytically solve the mass conservation equation to derive the well-known mean sediment concentration profile as a power-law of the distance to the sediment flow bed:

$$\frac{\langle \phi \rangle}{\phi_r} = \left(\frac{H_f - z}{z} \frac{z_r}{H_f - z_r} \right)^{Ro}, \quad (2)$$

with ϕ_r a reference concentration taken at an elevation z_r and

$$Ro = S_c W_s^0 / \kappa u_*, \quad (3)$$

the Rouse number corresponding to the slope of the particle concentration profile.

Discrepancies between a measured concentration profile and the Rouse profile have been attributed to a modification of the particle diffusivity compared with the eddy viscosity, leading to values of the turbulent Schmidt number S_c different from unity. The classical method estimates the Schmidt number by best fitting the measured concentration profile with the Rouse profile and leaving

S_c as the only free parameter. The resulting S_c is a depth-averaged value noted $\overline{S_c}$ in the following. Figure 1a summarizes several data-sets reported in the literature [11] for $\overline{S_c}$ values as a function of W_s/u_* . The first observation that can be made is the large scatter of the data with values lower and higher than unity. Values lower (higher) than unity can be interpreted as an enhanced (reduced) dispersion of particles compared to fluid momentum. van Rijn [15] suggested that turbulent dispersion of inertial particles is enhanced due to centrifugal force which tends to throw particles out of small-scale turbulent vortices and proposed an empirical model (see appendix A). While this model (solid line in Figure 1a) is widely used, it does not match the laboratory data of [9].

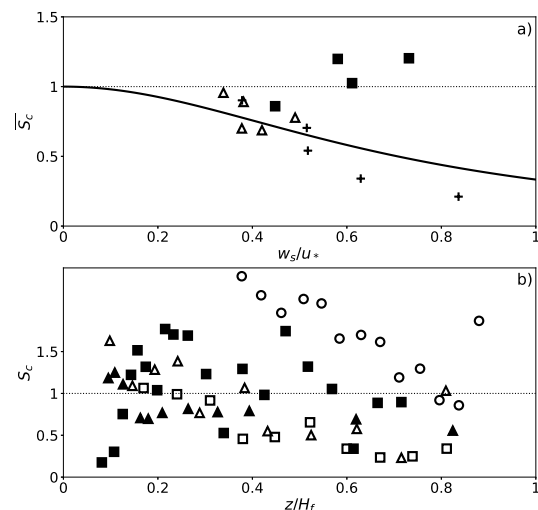


FIG. 1. Experimental data for the turbulent Schmidt number S_c from [11]: a) Averaged values of S_c over $0.1 < z/H_f < 0.5$ as a function of W_s^0/u_* : \triangle [7] run 36, $+$ [8], \blacksquare [9] b) Local estimates of S_c for uniform flow over a plane equilibrium bed as a function of relative distance, z/H_f , from the bed: \circ [10] run SAT S015, \blacksquare [9] run EQ2565, \blacktriangle [9] run EQ1665, \square [7] run 31, \triangle [7] run 36.

The turbulent Schmidt number can also be obtained locally provided that the concentration profile is measured with enough accuracy to resolve the sharp wall-normal gradients near the flow bed. Figure 1b shows a summary of existing data for this quantity as a function of the depth z/H_f . Again S_c shows large scatter with values ranging from as low as 0.2 to as large as 2.5. In some experiments [7, 9], only the mean concentration is measured and S_c is obtained using the same assumptions as $\overline{S_c}$ with $W_s = W_s^0$. In others, [10, 16], using an acoustic particle flux profiler the authors measured directly the Reynolds particle flux. It is interesting to point out that almost all data points (circles in 1b) suggest $S_c > 1$.

The potential reasons for the discrepancies in the Schmidt number values reported in the literature are (i) the assumption of particle settling velocity in quiescent water for the settling flux in Eq. (1) and (ii) the assumption of the von Karman constant value being identical to the clear water value ($\kappa = 0.41$). Concerning the first assumption, it has been shown in the literature that the settling velocity of individual particles could be modified in turbulent flows [18–23]. However, no consensus has been reached on the effect of turbulence on the settling velocity of individual particles, some studies have found settling enhancement while others observed settling retardation [24]. Regarding the second assumption, it has been reported in the literature [12, 13, 25] that the von Karman constant κ can be significantly reduced in certain flow conditions (up to a factor 2). Two physical mechanisms have been proposed to explain this reduction, density stratification [26] and/or turbulent drag work [14, 27]. The fact that the ratio S_c/κ appears in the Rouse number definition (Eq. 3) could explain some of the observed discrepancies in the literature. It is possible that the reported turbulent Schmidt number lower than unity is due to a decrease of κ . In order to elucidate the science question raised in this letter, it is mandatory to measure concurrently and with enough accuracy the velocity and concentration profiles to allow for a direct estimate of the von Karman constant and of the turbulent Schmidt number. This ability represents a major measurement challenge under such highly turbulent and energetic particle-laden boundary layer flow conditions.

To the best of our knowledge, the first measurements reported in the literature showing turbulent fluxes, mean concentration and velocity profiles are those of [16] using their Acoustic Particle Flux Profiler. Over the past ten years, we have intensively developed and improved this technology as the Acoustic Concentration and Velocity Profiler (ACVP) offering a unique wide-band multi-frequency capability for simultaneous vertical profiles of velocity and particle concentration at turbulence resolving scales ($\Delta z = o(1)$ mm ; $f \approx 80$ Hz) and across both the dilute suspension and the dense bedload layers [28–32]. We successfully applied this technology to study intense sediment transport processes in the so-called sheet-flow regime in [12, 13]. This unique data-set allows for the first time to investigate the relationship between Reynolds particle flux, Reynolds stress, and velocity and particle concentration gradients in order to shed new light on the turbulent Schmidt number value (see Appendix B for details).

On the numerical modeling side, significant progress has also been made over the last two decades regarding the understanding of particle transport processes using two-phase flow approaches [33–36]. Recently, we have performed the first turbulence-resolving two-fluid simulation for intense sediment transport regime [14] that has been validated against experimental data from [12, 13]. In this approach, the most energetic turbulent flow scales are directly resolved as well as the particle dynamics al-

lowing to simulate the turbulent particle fluxes across both the dilute suspension and dense bedload layers (see Appendix C for details).

In the following our unique high-resolution experimental data, denoted as RB15, and two-fluid turbulence-resolving simulation results, denoted as two-fluid LES (Large Eddy Simulation), are analyzed to infer whether $S_c > 1$ or $S_c < 1$ (see table I).

TABLE I. A summary of experimental parameters. Particle diameter (d_p), settling velocity (W_s^0), friction velocity (u_*), suspension number ($S = W_s^0/u_*$), bulk Reynolds number ($Re_b = UH_f/\nu$), with $\nu = 10^{-6}m^2/s$, particulate Reynolds number ($Re_p = W_s^0d_p/\nu$) and Stokes number ($St = \tau_p/\tau_\eta$) with $\tau_p = \rho_p d_p^2/(18\rho_f\nu)$ the particle response time and $\tau_\eta = \eta^2/\nu$ the Kolmogorov time-scale. RB15 was published in [12, 13] and SL99run1 and SL99run2 were published in [16].

Runs	d_p (mm)	$\frac{\rho_p}{\rho_f}$	W_s^0 (cm/s)	u_* (cm/s)	$\frac{W_s}{u_*}$	Re_b ($\times 10^4$)	Re_p	St
RB15	3	1.19	6.2	5.0	1.2	9	186	17.4
SL99run1	0.13	2.65	1.2	4.8	0.25	26	1.3	1.9
SL99run2	0.13	2.65	1.2	5.2	0.23	29	1.3	2.2

In order to avoid any uncertainties associated with a modification of the von Karman constant, the eddy viscosity is calculated directly as:

$$\nu^t = \frac{|\langle u'w' \rangle|}{\frac{d\langle u \rangle}{dz}}. \quad (4)$$

To better illustrate the change in the von Karman constant value, figure 2b presents the turbulent mixing length $l_m = \sqrt{|\langle u'w' \rangle|/d\langle u \rangle/dz}$. As pointed out in [12], the von Karman constant value obtained in the experiment is $\kappa \approx 0.225$, a significantly lower value than 0.41 expected for clear water flow conditions. The two-fluid LES perfectly reproduces this reduction. In [14] it is demonstrated that this reduction is due to the turbulent drag work. This modification of the von Karman "constant" value, usually assumed to be unaffected by the presence of particles, has significant fundamental consequences for boundary layer modeling in particle-laden flows. Furthermore, as the von Karman "constant" appears at the denominator of the Rouse number, its value also severely impacts suspended particle transport.

The classical method to estimate the turbulent Schmidt number is indirect and assumes a local balance between the gradient-diffusion model (Eq. (1)) and the gravity-driven settling flux $W_s^0\phi$:

$$S_{w\phi} = \frac{\nu^t}{W_s^0\langle\phi\rangle} \left| \frac{d\langle\phi\rangle}{dz} \right|. \quad (5)$$

This quantity will be denoted as $S_{w\phi}$ and is shown in figure 2c. For $z/H_f \gtrsim 0.1$, $S_{w\phi}$ is more or less constant

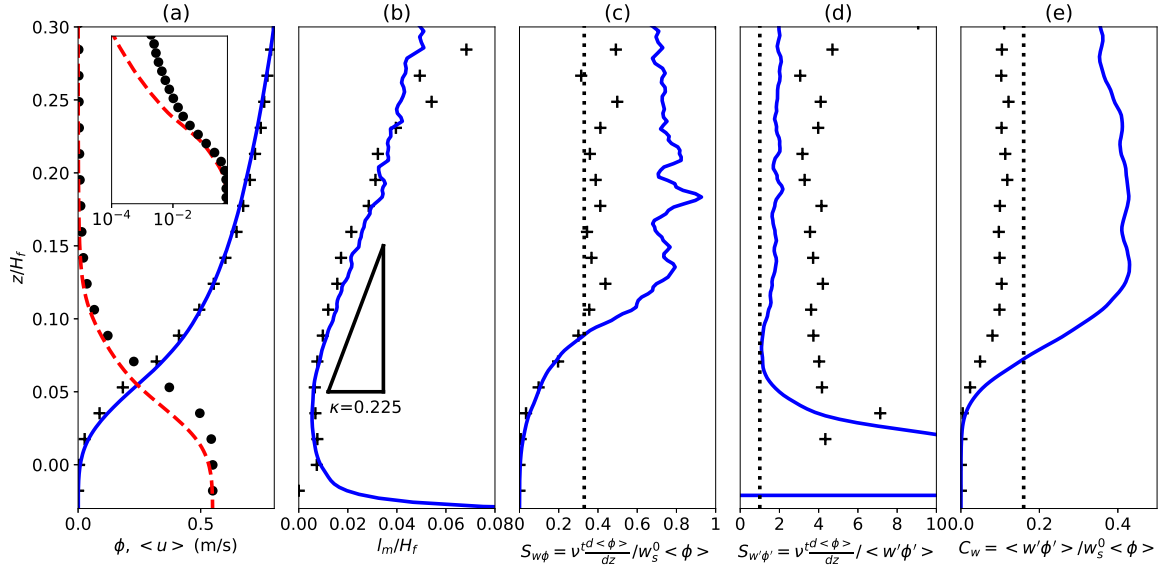


FIG. 2. Measured data (+, •) and LES results (—, - -) for vertical profiles of (a) velocity and concentration (b) mixing length, (c) Schmidt number defined according to [6] hypothesis $S_{w\phi} = -\nu^t d\langle\phi\rangle/dz/W_s^0\langle\phi\rangle$ Eq. (5) (dotted line corresponds to the empirical model [15]: $S_{w\phi} = 0.33$ Eq. (??)), (d) Schmidt number based on the resolved Reynolds flux $S_{w'\phi'} = \nu^t d\langle\phi\rangle/dz/\langle w'\phi'\rangle$ Eq. (6) (dotted line represents a Schmidt number equal to unity) (e) ratio between the wall-normal particle flux and the gravity driven particle flux based on the settling velocity in clear water: $C_w = \langle w'\phi'\rangle/W_s^0\langle\phi\rangle$ Eq. (7) (dotted line corresponds to [23] empirical formula: $W_s^e/W_s^0 = 0.16$ Eq. (??)).

with a value below unity $S_{w\phi} \approx 0.4$ for RB15 data and $S_{w\phi} \approx 0.7$ for two-fluid LES. The model proposed by [15] (see Eq. 4 in appendix A) gives a value of $\overline{S_c} = 0.3$ which is very close to the experimental value.

The direct method is based on the measured or simulated eddy viscosity and Reynolds particle flux. Using these quantities, the turbulent Schmidt number can be calculated without additional assumptions as:

$$S_{w'\phi'} = \frac{\nu^t}{\langle w'\phi'\rangle} \left| \frac{d\langle\phi\rangle}{dz} \right|. \quad (6)$$

This quantity will be denoted as $S_{w'\phi'}$ and is shown in figure 2d. The profiles are almost constant for $z/H_f \geq 0.1$, and the measured $S_{w'\phi'}$ is about 4 in RB15 while the two-fluid LES gives a lower value of about 1.7, confirming a value well above unity. As mentioned above, measurement of the Reynolds particle flux $\langle w'\phi'\rangle$ remains a particularly challenging task which, to the best of the authors knowledge, has only been provided to date in [16] and [12, 13].

In multi-phase flow approach, it is well-known that inertial particles cannot respond instantaneously to the wide range of fluid velocity fluctuations in a highly turbulent flow and that their dynamics can be significantly different from that of the fluid parcels [1]. Particle inertia is estimated using the particle Stokes number $St = \tau_p/\tau_\eta$ where τ_η is the Kolmogorov time-scale associated with the smallest turbulent eddies. Inertial particles corresponds to $St > 1$ which is the case for the configurations

investigated herein (see table I). This supports the observation that turbulent dispersion of particles should be less efficient than turbulent mixing of fluid momentum $S_{w'\phi'} > 1$. Therefore, the indirect estimate of turbulent Schmidt number lower than unity $S_{w\phi} < 1$ can only be explained by the need to further include vertical mass balance and uncertainties in estimating settling velocity using W_s^0 . In other words, the settling velocity in turbulent water has to be lower than that in quiescent water to explain RB15 measurements. In a recent paper, using the exact same particles as in RB15, [23] have shown that the settling velocity of an isolated particle falling in an homogeneous isotropic turbulent flow field can be as low as 50% of its value in quiescent water.

In order to investigate this point, an effective settling velocity W_s^e is defined from the mass balance equation, as:

$$W_s^e = \frac{\langle w'\phi'\rangle}{\langle\phi\rangle}. \quad (7)$$

Dividing this value by W_s^0 a dimensionless settling velocity $C_w = W_s^e/W_s^0$ is obtained. This quantity is plotted in figure 2e which shows an almost constant value in the dilute suspended-load layer ($z/H_f \geq 0.1$) for both RB15 and two-fluid LES results. The measured quantity shows that the effective settling velocity is about ten times smaller than the one in quiescent water *i.e.* $C_w \approx 0.1$ consistent with measurements of [23] (see Appendix D for details). The two-fluid LES also predicts settling retardation even though the reduction is less strong ($C_w = 0.4$)

than in RB15 experiments. Despite the discrepancy in magnitude, both numerical and measured values strongly support the hypothesis that settling retardation is responsible for the indirectly measured Schmidt number value smaller than unity.

In order to verify our hypothesis, the measured data reported by [16] (see table I) are further examined using the same methodology as described above. The hydrodynamic conditions of these two runs (red and green symbols in Figure 3) are very similar to RB15 flow conditions in terms of bed-slope, water discharge, flow depth, bed friction velocity, Reynolds number values, the major differences concern the particles properties that are denser and smaller and the suspended particle concentration which was two order of magnitude smaller.

Figure 3b shows the mixing length profiles, the triangle indicates the slope for a von Karman constant value equal to 0.41. It can be seen that the spatial resolution in [16] is more than 3 times coarser than in RB15 with more scattered data. Nevertheless, it appears that the slope of the mixing length profile is clearly higher with a value closer to the clear water value. This suggests that for finer particles and lower suspended particle concentration no reduction of the von Karman constant is observed. In figure 3c, the turbulent Schmidt number $S_{w\phi}$ shows the same trend as for RB15 in the near wall region where the value is lower than unity but the scatter in [16] increases away from the wall where $S_{w\phi}$ exceeds unity. The vertical profiles of $S_{w'\phi'}$ are shown in figure 3d. All data reveal values well above unity supporting lower turbulent particle diffusivity compared to eddy viscosity. Finally, the vertical profile of the dimensionless settling velocity C_w is shown in figure 3e. Both runs exhibit a value smaller than unity confirming the hypothesis of settling retardation but with a weaker magnitude. Furthermore, the C_w profiles increase linearly with distance from the bed whereas the RB15 data exhibit a fairly constant value. These differences may probably be attributed to the differences in Stokes number and particulate Reynolds number values but this would deserve further investigation.

In summary, the results presented herein reveals that, for inertial particles, the turbulent Schmidt number is larger than unity. Measurements and two-fluid LES re-

vealed that for the large lightweight particles (RB15) the von Karman constant is significantly reduced (factor 2) and strong settling retardation occurs (10% of the quiescent water value) with a fairly constant magnitude in the dilute suspension layer. For dilute fine sands suspensions (SL99Run1 & 2) the von Karman constant seems almost unaffected, settling retardation is also observed but with a magnitude decreasing with distance from the bed.

In conclusion, thanks to our innovative highly-resolved measurement technique and numerical simulations we have been able to obtain an exciting result that completely changes the paradigm of suspended inertial particle transport by a boundary layer flow. We have demonstrated that (i) turbulent dispersion of inertial particles in a boundary layer flow is significantly smaller than that of fluid parcels and does not depend much on particle size and density and (ii) settling velocity of inertial particles is reduced and this reduction depends on particle size and density. This suggests that the particle properties are sensitive parameters in this problem but the details of the underlying physical mechanisms are still to be elucidated. Beyond the importance for sediment transport predictions, these findings are relevant to a wide range of two-phase flows involving inertial particle transport such as avalanches, turbidity currents, pneumatic transport and particle deposition in material processing.

ACKNOWLEDGMENTS

The authors would like to thank N. Mordant and P. Frey for their comments on the manuscript.

J. Chauchat is supported by the french ANR project SHEET-FLOW (ANR-18-CE01-0003). D. Hurther is supported by the french DGA-funded ANR Astrid Maturation project MESURE (ANR-16-ASMA-0005). Z. Cheng and T.-J. Hsu are supported by U.S. Strategic Environmental Research and Development Program (SERDP, MR20-1478) and National Science Foundation (OCE-1635151). The computations presented in this paper were performed using the GENCI infrastructure under Allocations A0060107567 and A0080107567 and the GRICAD infrastructure.

-
- [1] S. Balachandar and J. K. Eaton, Turbulent dispersed multiphase flow, *Annual Review of Fluid Mechanics* **42**, 111 (2010).
 - [2] M. Garcia, *Sedimentation Engineering* (American Society of Civil Engineers, 2008) <https://ascelibrary.org/doi/pdf/10.1061/9780784408148>.
 - [3] T. Aagaard and M. G. Hughes, Breaker turbulence and sediment suspension in the surf zone, *Marine Geology* **271**, 250 (2010).
 - [4] L. Prandtl, Bericht über neuere Turbulenzforschung, *Hydraulische Probleme. Vorträge Hydrauliktagung* Göttingen **5**, 1 (1926).
 - [5] V. A. Vanoni, *Sedimentation engineering* (Am. Soc. Coastal Eng., 1975).
 - [6] H. Rouse, Experiments on the mechanics of sediment suspension, in *ICAM* (1938) pp. 550–554.
 - [7] J. R. Barton and P.-N. Lin, *A study of the sediment transport in alluvial streams*, Tech. Rep. (Civil Engineering Dept., Colorado A & M College, Fort , Colorado, 1955).
 - [8] N. L. Coleman, Flume studies of the sediment transfer coefficient, *Water Resour. Res.* **6**, 801 (1970).
 - [9] D. A. Lyn, A similarity approach to turbu-

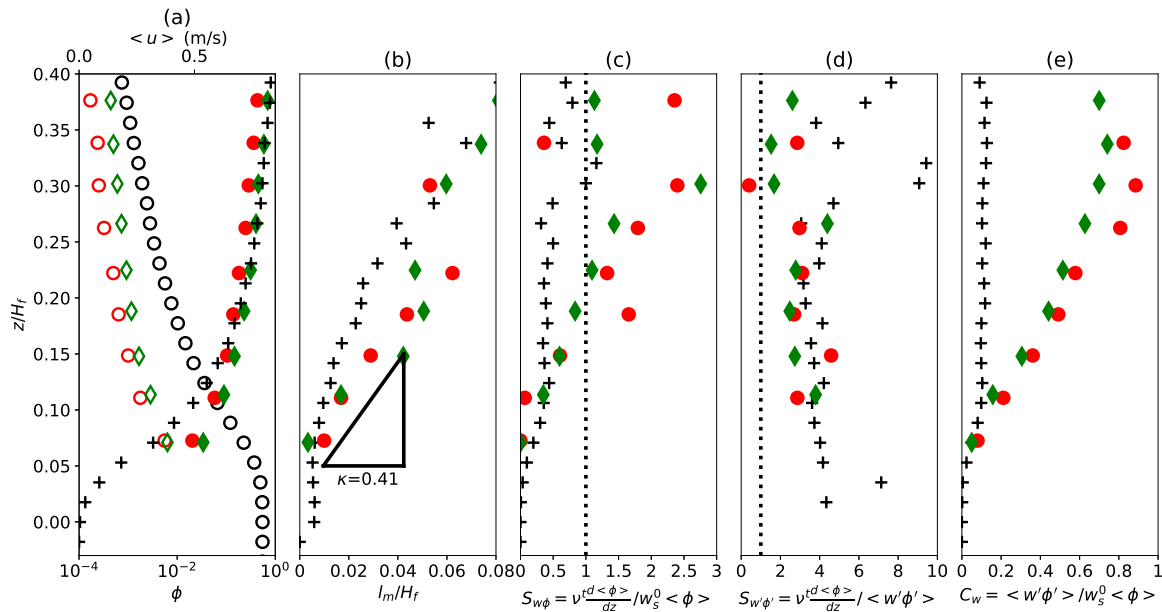


FIG. 3. Comparison of RB15 data with [16] data reported for two different hydrodynamic conditions noted SL99run1 (red circle \circ) and SL99run2 (green diamond \diamond): (a) velocity and concentration profiles (b) mixing length, (c) Schmidt number defined according to [6] hypothesis $S_{w\phi} = -\nu^t d\langle\phi\rangle/dz/W_s^0\langle\phi\rangle$ Eq. (5), (d) Schmidt number based on the resolved Reynolds flux $S_{w\phi'} = \nu^t d\langle\phi\rangle/dz/\langle w'\phi'\rangle$ Eq. (6) (dotted line represents a Schmidt number equal to unity) (e) dimensionless settling velocity in C_w .

- lent sediment-laden flows in open channels, *Journal of Fluid Mechanics* **193**, 1 (1988).
- [10] M. Cellino and W. H. Graf, Sediment-laden flow in open-channels under noncapacity and capacity conditions, *Journal of Hydraulic Engineering* **125**, 455 (1999).
- [11] D. A. Lyn, Turbulence models for sediment transport engineering, in *Sedimentation Engineering* (ASCE, 2008) Chap. Chapter 16.
- [12] T. Revil-Baudard, J. Chauchat, D. Hurther, and P.-A. Barraud, Investigation of sheet-flow processes based on novel acoustic high-resolution velocity and concentration measurements, *Journal of Fluid Mechanics* **767**, 1 (2015).
- [13] T. Revil-Baudard, J. Chauchat, D. Hurther, and O. Eiff, Turbulence modifications induced by the bed mobility in intense sediment-laden flows, *Journal of Fluid Mechanics* **808**, 469 (2016).
- [14] Z. Cheng, T.-J. Hsu, and J. Chauchat, An eulerian two-phase model for steady sheet flow using large-eddy simulation methodology, *Advances in Water Resources* **111**, 205 (2018).
- [15] L. C. Van Rijn, Sediment transport, part ii: Suspended load transport, *J. Hydraul. Eng.* **110**, 1613 (1984).
- [16] C. Shen and U. Lemmin, Application of an acoustic particle flux profiler in particleladen open-channel flow, *Journal of Hydraulic Research* **37**, 407 (1999), <https://doi.org/10.1080/00221686.1999.9628256>.
- [17] M. Cellino, *Experimental study of suspension flow in open channels*, Ph.D. thesis, Swiss Federal Institute of Techn. Lausanne (1998).
- [18] S. P. Murray, Settling velocities and vertical diffusion of particles in turbulent water, *Journal of Geophysical Research* **75**, 1647 (1970).
- [19] G. H. Good, P. J. Ireland, G. P. Bewley, E. Bodenschatz, L. R. Collins, and Z. Warhaft, Settling regimes of inertial particles in isotropic turbulence, *Journal of Fluid Mechanics* **759**, R3 (12 pages) (2014).
- [20] A. J. Cuthbertson and D. A. Ervine, Experimental study of fine sand particle settling in turbulent open channel flows over rough porous beds, *Journal of Hydraulic Engineering* **133**, 905 (2007).
- [21] K. Kawanisi and R. Shiozaki, Turbulent effects on the settling velocity of suspended sediment, *Journal of Hydraulic Engineering* **134**, 261 (2008).
- [22] Q. Zhou and N.-S. Cheng, Experimental investigation of single particle settling in turbulence generated by oscillating grid, *Chemical Engineering Journal* **149**, 289 (2009).
- [23] Y. Akutina, T. Revil-Baudard, J. Chauchat, and O. Eiff, Experimental evidence of settling retardation in a turbulence column, *Physical review of Fluids* **5** (2020).
- [24] P. Nielsen, *Coastal Bottom Boundary Layers and Sediment Transport* (WORLD SCIENTIFIC, 1992) <https://www.worldscientific.com/doi/pdf/10.1142/1269>.
- [25] V. Vanoni, Some experiment on the transporation of suspended load, *Eos, Transactions American Geophysical Union* **22**, 608 (1941).
- [26] C. Vilaret and A. G. Davies, Modelling of sediment-turbulent flow interactions, *Applied Mechanics Review* **48**, 601 (1995).
- [27] T. Hsu, J. T. Jenkins, and L. F. Liu, On two-phase sediment transport: Dilute flow, *J. Geophys. Res.* **108**, 14 (2003).
- [28] D. Hurther, P. D. Thorne, M. Bricault, U. Lemmin, and J.-M. Barnoud, A multi-frequency acoustic concentration and velocity profiler (acvp) for boundary layer measure-

- ments of fine-scale flow and sediment transport processes, *Coastal Engineering* **58**, 594 (2011).
- [29] D. Hurther and P. D. Thorne, Suspension and near-bed load sediment transport processes above a migrating, sand-rippled bed under shoaling waves, *Journal of Geophysical Research: Oceans* **116**, n/a (2011).
- [30] S. Naqshband, A. J. F. Hoitink, B. McElroy, D. Hurther, and S. J. M. H. Hulscher, A sharp view on river dune transition to upper stage plane bed, *Geophysical Research Letters* **44**, 11,437 (2017),.
- [31] G. Fromant, R. S. Mieras, T. Revil-Baudard, J. A. Puleo, D. Hurther, and J. Chauchat, On bedload and suspended load measurement performances in sheet flows using acoustic and conductivity profilers, *Journal of Geophysical Research: Earth Surface* **123**, 2546 (2018).
- [32] G. Fromant, D. Hurther, J. van der Zanden, D. A. van der A, I. Cáceres, T. O'Donoghue, and J. S. Ribberink, Wave boundary layer hydrodynamics and sheet flow properties under large-scale plunging-type breaking waves, *Journal of Geophysical Research: Oceans* **124**, 75 (2019).
- [33] S. K. Jha and F. A. Bombardelli, Toward two-phase flow modeling of nondilute sediment transport in open channels, *J. Geophys. Res.* **115** (2010).
- [34] T. Revil-Baudard and J. Chauchat, A two-phase model for sheet flow regime based on dense granular flow rheology, *Journal of Geophysical Research: Oceans* **118**, 619 (2013).
- [35] C.-H. Lee, Y. M. Low, and Y.-M. Chiew, Multi-dimensional rheology-based two-phase model for sediment transport and applications to sheet flow and pipeline scour, *Physics of Fluids* **28**, 053305 (2016), <http://dx.doi.org/10.1063/1.4948987>.
- [36] Z. Cheng, T.-J. Hsu, and J. Calantoni, Sedfoam: A multi-dimensional eulerian two-phase model for sediment transport and its application to momentary bed failure, *Coastal Engineering* **119**, 32 (2017).
- [37] J. R. Finn and M. Li, Regimes of sediment-turbulence interaction and guidelines for simulating the multiphase bottom boundary layer, *International Journal of Multiphase Flow* **85**, 278 (2016).